Estimating Chromaticity of Multicolored Illuminations

Robby T. Tan Katsushi Ikeuchi

Department of Computer Science
The University of Tokyo

{robby,ki}@cvl.iis.u-tokyo.ac.jp

Abstract

In machine vision, many methods have been developed to estimate illumination color. But, few of these methods deal with multicolored illuminations. To our knowledge, no method that uses highlights as a main part to analyze has been proposed for the purpose of handling multicolored illuminations. Although several methods can be applied for that purpose, they need a separate process for each highlight region that has the same illumination color. This requirement is problematic for textured surfaces since, in different surface colors, whether two regions of highlight have the same illumination color is difficult to determine. In this paper, we introduce a method that can handle both single- and multi-colored illuminations. The method is principally based on inverse-intensity chromaticity space, a two-dimensional space that was originally proposed to estimate a single color of illumination. We extend the usage of the space by developing an iterative algorithm to deal with multicolored illuminations. The method requires only crude highlight regions of all illumination colors, without requiring any further segmentation process. Moreover, the method is still feasible even if the number of illumination colors is unknown.

1. Introduction

Color appearance of an object is dependent on the color of the illumination. When the illumination color changes, the color appearance of an object will change accordingly. This color inconsistency causes many algorithms in computer vision to produce erroneous results. To overcome this problem, an algorithm to estimate and reduce illumination color or usually called color constancy is required. Moreover, once the illumination color is reduced, the object *actual* color becomes identifiable.

In machine vision, many methods have been developed to estimate illumination color. But, few of these methods deal with multicolored illuminations. In this paper, we describe how, by analyzing all highlight regions simultaneously, we achieve our goal of estimating chromaticity of multicolored illuminations. This goal is motivated by the fact that the presence of illumination with different colors is, in some situations, inevitable.

Generally, based on the reflection model they use, color constancy methods can be categorized into two classes: diffuse-based and dichromatic-based methods. Diffuse-based methods [3, 5, 8, 18, 22, 12, 11] assume that the input image has diffuse only reflection. Consequently, the presence of specular reflection will cause the methods to produce erroneous results. Most statistics-based color constancy methods (a term coined by Finlayson *et al.* [10]) base their algorithm on diffuse only reflection. On the other hand, dichromatic-based methods [4, 6, 15, 16, 1, 20] assume that the input image has both diffuse and specular reflection components. Since specular reflection has more clues to estimate illumination color, in general, compared to diffuse-based methods, dichromatic-based methods produce more accurate results.

Methods in dichromatic-based color constancy rely on the dichromatic reflection model proposed by Shafer [19]. Klinker *et al*. [13] introduced a method to estimate illumination color from a uniformly colored surface by extracting a T-shape color distribution in the RGB space. Lee [15] proposed a method to estimate illumination chromaticity using highlights of at least two surface colors. The estimation is accomplished by finding an intersection point of two or more dichromatic lines in chromaticity space. Parallel to this, many methods have been proposed in the literature [4, 21, 23, 9, 10].

The aforementioned methods were originally proposed to handle a single color of illumination. Although several dichromatic-based methods can be applied to handle multicolored illuminations, they require a separate process for each highlight region whose illumination color is the same. This requirement is problematic for textured surfaces since, in different surface colors, whether two regions of highlight have the same illumination color is difficult to determine. Few methods have been intentionally proposed to handle multicolored illuminations. Land *et al*. [14] introduced a retinex theory to estimate illumination colors in a matte and plane surface. Their theory is principally based on the assumption that the intensity change of surface color is larger than that of illumination color. Finlayson *et al*. [7] introduced a method that uses a single surface color illuminated by two different illumination colors. The main idea of their approach is that, given two different reflected lights (pixels) produced by the same surface color but different illumination colors, then by dividing the first pixel with all possible illumination colors (in which the illumination color that illuminates the first pixel exists) and intersecting to the second pixel that is also divided by all possible illumination

colors will produce an intersection point representing the actual surface color. Barnard *et al*. [2] utilized the retinex algorithm [14] to automatically obtain a surface color with different illumination color, and then used the method of Finlayson *et al*. [7] to estimate varying illumination colors. Recently, Andersen *et al*. [1] developed a method to asses the illumination condition covering two light sources. The method provides an analysis of image chromaticity under two illumination colors for dichromatic surfaces.

Most color constancy methods, besides having problems with the number of illumination colors, also have problems with the number of surfaces colors. Most of them cannot handle both uniformly colored surfaces and highly textured surfaces in a single integrated framework. Statistics-based methods require many surface colors, and become error prone when there are only few surface colors. In contrast, dichromatic-based methods can successfully handle uniformly colored surfaces, but cannot be applied to highly textured surfaces since they require precise color segmentation [20]. Fortunately, this problem can be resolved by utilizing inverse-intensity chromaticity space introduced by Tan *et al.* [20]. The space is effective to estimate illumination chromaticity for both uniformly colored surfaces and highly textured surfaces. However, in [20], the space was proposed solely to estimate a single color of illumination.

In this paper, we extend the usage of inverse-intensity chromaticity space to handle multicolored illuminations by retaining its capability to handle various numbers of surface colors. The basic idea of our method is to remove specular clusters that have the same illumination color in the space one by one iteratively while estimating each illumination color. Given crude highlight regions, this process is done without requiring any segmentation process. In inverse-intensity chromaticity space, Tan *et al.* found that specular clusters are composed of straight lines that head for a certain value at y-axis, which the value is identical to illumination chromaticity. Thus, by finding each straight line using the Hough transform, we can remove each cluster that has the same illumination color. Moreover, we do not assume that the number of illumination colors is known. As a result, besides estimating illumination chromaticity, the method is also able to estimate the number of illumination colors. We set our analysis on highlight regions that can be obtained by thresholding the intensity and saturation values following the method proposed by Lehmann *et al.* [17]. While the ability to work on rough estimates of highlight regions is one of the advantages of our method, the highlight regions identification is still an open challenging problem. In addition, since no assumption of the illumination chromaticity is used, the method is also effective for all possible colors of illumination.

The rest of the paper is organized as follows: in Section 2, image color formation of inhomogeneous materials is discussed. In Section 3, we first review inverse-intensity chromaticity space, and then explain the usage of the space to handle multicolored illuminations. We provide experimental results for real images in Section 4. Finally in Section 5, we conclude our paper.

2 Reflection Model

An image of dielectric inhomogeneous objects taken by a digital color camera, according to the dichromatic reflection model [19], can be described as:

$$I_c(\mathbf{x}) = w_d(\mathbf{x}) \int_\Omega S(\lambda,\mathbf{x})E(\lambda,\mathbf{x})q_c(\lambda)d\lambda + w_s(\mathbf{x}) \int_\Omega E(\lambda,\mathbf{x})q_c(\lambda)d\lambda \quad (1)$$

where $\mathbf{x} = \{x, y\}$, the two dimensional image coordinates; $w_d(\mathbf{x})$ and $w_s(\mathbf{x})$ are the weighting factors for diffuse and specular reflection, respectively; their values depend on the geometric structure at location $\mathbf{x}$. $S(\lambda, \mathbf{x})$ is the spectral reflectance function; $E(\lambda, \mathbf{x})$ is the spectral energy distribution function of the illumination; q_c is the three-element-vector of sensor sensitivity and index c represents the type of sensors (r, g, and b). The integration is done over the visible spectrum (Ω). Note that we ignore the camera noise and gain in the above equation.

For the sake of simplicity, equation (1) is written as:

$$I_c(\mathbf{x}) = w_d(\mathbf{x})B_c(\mathbf{x}) + w_s(\mathbf{x})G_c(\mathbf{x}) \quad (2)$$

where $B_c(\mathbf{x}) = \int_\Omega S_d(\lambda,\mathbf{x})E(\lambda,\mathbf{x})q_c(\lambda)d\lambda$; and $G_c(\mathbf{x}) = \int_\Omega E(\lambda,\mathbf{x})q_c(\lambda)d\lambda$. The first part of the right side of the equation represents the diffuse reflection component, while the second part represents the specular reflection component.

3 Estimation Method

This section will be divided into two parts: first, a review of inverse-intensity chromaticity space to estimate a single illumination chromaticity, and second, an implementation of inverse-intensity chromaticity space to deal with multicolored illuminations using an iterative algorithm.

3.1 Inverse-intensity chromaticity space: a review

Inverse intensity chromaticity space [20] is principally based on the correlation between chromaticity and intensity. Chromaticity or also commonly called *normalized rgb* is defined as:

$$\sigma_c(\mathbf{x}) = \frac{I_c(\mathbf{x})}{\Sigma I_i(\mathbf{x})} \quad (3)$$

where $\Sigma I_i(\mathbf{x}) = I_r(\mathbf{x}) + I_g(\mathbf{x}) + I_b(\mathbf{x})$.

By considering the chromaticity definition (σ_c) in Equation (3) and image intensity definition (I_c) in Equation (2), for diffuse only reflection component ($w_s = 0$), the chromaticity becomes independent from the diffuse geometrical parameter w_d, since it is factored out by using Equation (3). We call this *diffuse chromaticity* (Λ_c) with definition:

$$\Lambda_c(\mathbf{x}) = \frac{B_c(\mathbf{x})}{\Sigma B_i(\mathbf{x})} \quad (4)$$

On the other hand, for specular only reflection component ($w_d = 0$), the chromaticity is independent from the specular geometrical parameter (w_s), which we call *specular chromaticity* (Γ_c):

$$\Gamma_c(\mathbf{x}) = \frac{G_c(\mathbf{x})}{\Sigma G_i(\mathbf{x})} \tag{5}$$

By considering Equation (4) and (5), consequently Equation (2) can be written as:

$$I_c(\mathbf{x}) = m_d(\mathbf{x})\Lambda_c(\mathbf{x}) + m_s(\mathbf{x})\Gamma_c(\mathbf{x}) \tag{6}$$

where

$$m_d(\mathbf{x}) = w_d(\mathbf{x})\Sigma B_i(\mathbf{x}) \tag{7}$$
$$m_s(\mathbf{x}) = w_s(\mathbf{x})\Sigma G_i(\mathbf{x}) \tag{8}$$

We can also set $\Sigma\sigma_i(\mathbf{x}) = \Sigma\Lambda_i(\mathbf{x}) = \Sigma\Gamma_i(\mathbf{x}) = 1$, without loss of generality. Note that, we assume the camera output is linear to the flux of incoming light intensity. Since, in our method, only using that assumption can the above chromaticity definitions be applied to estimate illumination chromaticity. As a result, we have three types of chromaticity: image chromaticity (σ_c), diffuse chromaticity (Λ_c) and specular chromaticity (Γ_c). The image chromaticity is directly obtained from the input image using Equation (3). In addition, based on the NIR assumption, we can regard the specular chromaticity (Γ_c) as illumination chromaticity.

By plugging the reflection equation (6) into the chromaticity definition (3), and by further derivation, a linear correlation of image chromaticity (σ_c), light chromaticity(Γ_c), and inverse intensity ($\frac{1}{\Sigma I_i}$) can be obtained:

$$\sigma_c = p\frac{1}{\Sigma I_i} + \Gamma_c \tag{9}$$

where $p = m_d(\Lambda_c - \Gamma_c)$. The equation is the most basic equation in the illumination chromaticity estimation method in [20]. It obviously shows that by knowing the values of p, the illumination chromaticity (Γ_c) can be directly determined, since σ_c and ΣI_i can be obtained from the input image. Hence, the problem is, how can we know the values of p which in most situations vary as they depends on m_d? Tan *et al.* [20] pointed out that in inverse intensity chromaticity space, specular points form a number of straight lines, where each line has a gradient which is identical to p. Figure 1.b shows the specular points of a synthetic image with a uniformly colored surface in inverse-intensity chromaticity space. By focusing on the specular cluster in Figure 1.b, they asserted, according to Equation 9, that the cluster is composed of a number of straight lines that head for the same value at y-axis as illustrated in Figure 3.a.

Figure 2.b shows the projection of highlighted regions of a synthetic image with a multicolored surface into inverse-intensity chromaticity space. The estimation process for multicolored surfaces is exactly the same as that for a uniformly colored surface since, instead of being concerned with each cluster, they were concerned with the direction of every straight line inside the clusters.

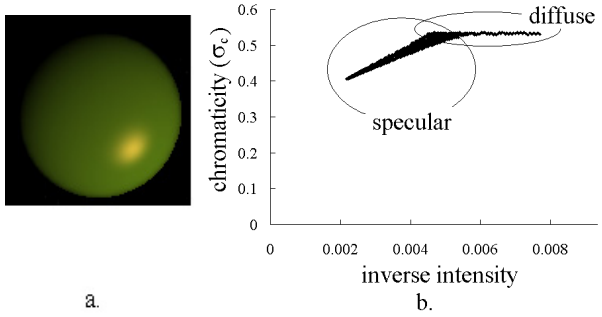

Figure 1: Synthetic image with uniformly colored surface. b. Projection of the diffuse and specular pixels into inverse-intensity chromaticity space, with σ_c representing the green channel

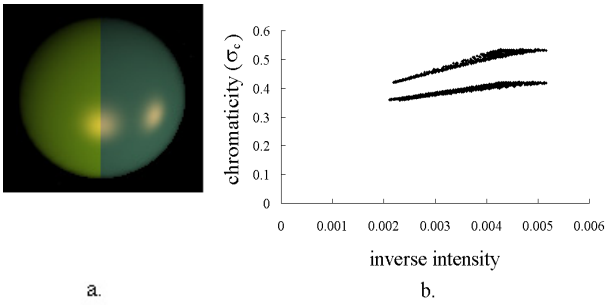

Figure 2: a. Synthetic image with two surface colors. b. Specular points in inverse-intensity chromaticity space, with σ_c representing the green channel

Hough transform and intersection counting To estimate the illumination chromaticity (Γ_c) from inverse-intensity chromaticity space, the method utilizes the Hough transform. Figure 4.a shows the transformation from inverse-intensity chromaticity space into the Hough space, where its x-axis represents Γ_c and its y-axis represents p. Since Γ_c is a normalized value, the range of its value is from 0 to 1 ($0 < \Gamma_c < 1$).

Using the Hough transform alone does not give a solution, because the values of p which are not constant throughout the image cause the intersection point of lines in the

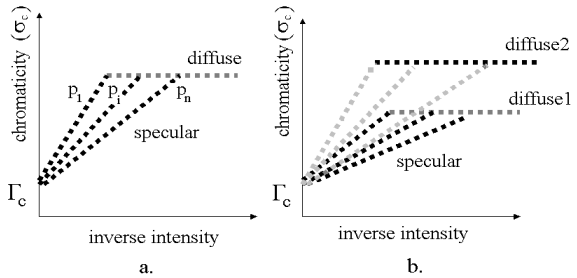

Figure 3: a. Sketch of specular points of a single surface color in inverse-intensity chromaticity space. b. Sketch of specular points of two surface colors in inverse-intensity chromaticity space.

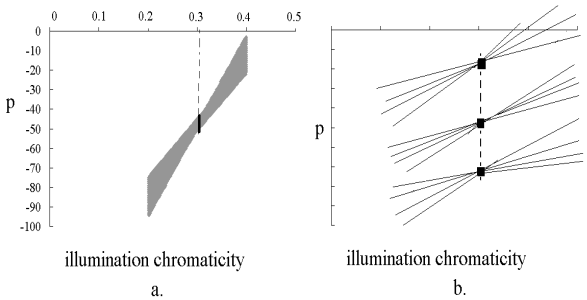

Figure 4: a. Projection of points in Figure 1.b into the Hough space. b. Sketch of intersected lines in the Hough space.

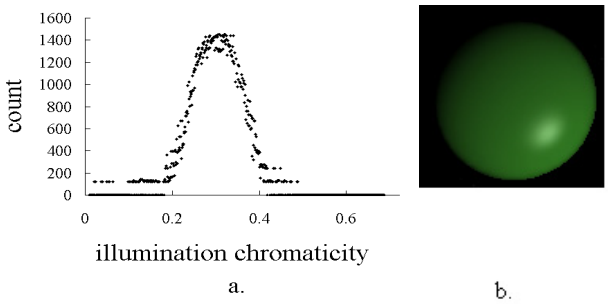

Figure 5: a. Intersections counting distribution in the green channel of chromaticity. b. Normalization result of the input synthetic image into pure white illumination with regard to the illumination chromaticity estimation. The estimated illumination chromaticity is as follows: $\Gamma_r = 0.5354$, $\Gamma_b = 0.3032$, $\Gamma_b = 0.1618$, the ground-truth values are: $\Gamma_r = 0.5358$, $\Gamma_b = 0.3037$, $\Gamma_b = 0.1604$

Hough space not to be located at a single location. Fortunately, even if the values of p vary, the values of Γ_c are constant. Thus, in principle, all intersections will be concentrated at a single value of Γ_c. These intersections are indicated by a thick solid line in Figure 4.a.

As a result, by projecting the total number of intersections of each Γ_c into a two-dimensional space, illumination-chromaticity count space, with y-axis representing the count of intersections and x-axis representing Γ_c, the actual value of Γ_c can be robustly estimated. Figure 5.a shows the distribution of the count numbers of intersections in the space, where the distribution forms a Gaussian-like distribution. The peak of the distribution lies at the actual value of Γ_c.

3.2 Multicolored Illuminations

In this subsection, we extend the usage of inverse-intensity space to handle multicolored illuminations. Theoretically, when an inhomogeneous object is lit by two light sources that have different color and sufficiently separated position, a certain surface region viewed from a certain position will exhibit highlight. This highlight, according to the Torrance-Sparrow reflection model [24], is mostly caused by one of the two illuminants. Thus, we can safely assume that the specular reflection component of a point on the surface is

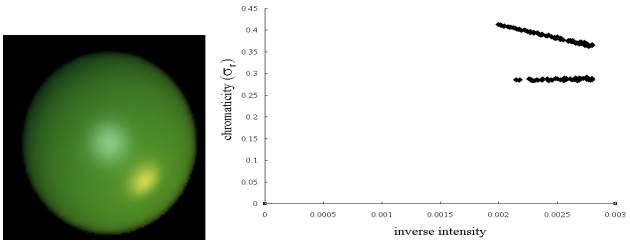

Figure 6: Synthetic image with a single surface color lit by two different colors of illuminants. b. Projection of the diffuse and specular pixels into chromaticity-intensity space, with σ_c representing the red channel

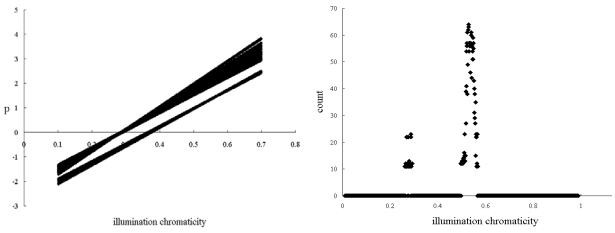

Figure 7: a. Projection of points in the red-channel inverse-intensity chromaticity space into the Hough space b. Intersection counting distribution in the red channel of chromaticity

identical to one of the illumination colors. Mathematically, it can be described as:

$$I_c(\mathbf{x}) = w_d \int_\Omega S(\lambda, \mathbf{x}) \Big[E_1(\lambda, \mathbf{x}) + E_2(\lambda, \mathbf{x}) \Big] q_c(\lambda) d\lambda + \int_\Omega E_1(\lambda, \mathbf{x}) q_c(\lambda) d\lambda \quad (10)$$

where E_1 and E_2 denote the first and second illumination colors, respectively.

The difference between Equation (10) and Equation (1) is the presence of the E_2 inside diffuse reflection component. This difference, fortunately, does not change the correlation described in Equation (9), since in inverse-intensity chromaticity space, E_2 does not affect the direction of the specular cluster; the direction is still determined by E_1. This phenomenon also occurs when more than two colors of illumination are present.

By projecting the pixels of an image lit by multicolored illuminations into inverse-intensity space, we will obtain several clusters that head in several directions instead of one direction, as shown in Figure 6.b. As a result, the Hough transform of the points in the space produces two clusters with different places of intersections (Figure 7.a). By counting the intersection distribution, we will obtain several peaks which the number depends on the number of illumination color, as shown in Figure 7.b.

Having observed the distribution in Figure 7.b, one may consider to find the peaks of the Gaussian-like distribution, in order to estimate the values of illumination chromaticity

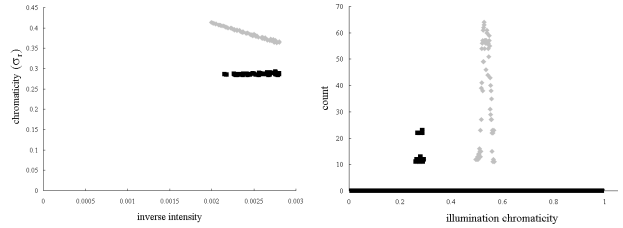

Figure 8: a. Second iteration in inverse intensity chromaticity space after identifying first illumination chromaticity. The brighter cluster is the pixels illuminated by the first illumination color b. Second iteration in intersection counting distribution in the red channel of chromaticity. The darker distribution is the distribution of second illumination chromaticity.

(Γ_c). While this direct solution probably works for synthetic images, unfortunately, it is extremely difficult for real images, since most real images suffer from noise, making the peak of one illumination color overlap with the distribution of other illumination colors. Another direct solution is to cluster all points in inverse-intensity chromaticity space using, for example, the nearest neighbors algorithm. Yet, even this solution is also a weak solution, since it leads to a segmentation problem, which is problematic if there are many surface colors as well as noise.

Iterative algorithm To overcome the problems, we devised a more accurate and robust approach by using an iterative algorithm. Pseudo-code (3.1) shows the underlying idea of the algorithm.

The detail of the algorithm is as follows. In the first step, like the method that handles a single illumination color, we project the highlight regions (N) into inverse-intensity chromaticity space (Figure 6.b). We transform the projection points into Hough space (Figure 7.a), and obtain the highest intersection counting in the illumination-chromaticity counting space (Figure 7.b). Then, we set the x-axis location of the highest counting as the first illumination chromaticity ($\Gamma_c[1]$).

In the second step, from the value of $\Gamma_c[1]$, we identify all values of $p[1]$ in the Hough space. By knowing both $\Gamma_c[1]$ and $p[1]$, in the next step we can identify the straight lines (points) in inverse-intensity chromaticity space heading for $\Gamma_c[1]$. Finally, we remove the pixels in N that its projection points heading for $\Gamma_c[1]$, which means remove all points that have illumination color identical to $\Gamma_c[1]$. The algorithm iteratively repeats the same process until there are no more points in N. Intuitively, Steps 2, 3, and 4 are inverse process of Step 1, whose purpose is to identify and to remove pixels that have the same illumination color. Figure 8.a show the projection of N after cluster lit by $\Gamma_c[1]$ is detected. The brighter cluster represents the detected cluster. In Figure 8.b, the darker points represents the intersection counting distribution of second illumination chromaticity.

Ideally, all processing can be done independently for each color channel; yet, for natural illumination, the range of green chromaticity values is very narrow. Consequently, identifying the values of $p[i]$ between two or more colors in the Hough space regarding the green channel will be error prone. To overcome the problem, from Step 2 until Step 4, the processes are accomplished with regard to one color channel. In our implementation we chose the red channel, since for natural illuminants, this channel has a wide range of illumination chromaticity values.

Algorithm 3.1: ITERATION(N)

comment: N= highlight regions

comment: IIC=inverse intensity chromaticity

$i = 0$
while $(sizeof(N) > \epsilon)$
- (1) project N into IIC space
  - (a) transform points in ICC space into Hough space
  - (b) count the histogram of the intersections
  - (c) find the highest intersection counting
  - (d) set the highest intersection's x-axis equal to $\Gamma_c[i]$
- (2) based on $\Gamma_c[i]$, search all values of $p[i]$ in Hough space
- (3) based on $\Gamma_c[i]$ and values of $p[i]$ identify points in IIC space
- (4) based on identified points in IIC space remove pixels in image N
- i++

comment: $\epsilon \approx 0$

return (i, Γ_i)
comment: i = the number of illumination colors

Note that, in this paper, we assume that the light sources' positions are not parallel and sufficiently distant to each other, so that one region of a specular reflection component has only one illumination color. In other words, we do not intend to handle highlights that contain two or more illumination colors (color-blended highlights). However, as in the real world, it is difficult to avoid such a condition, our implementation is tolerant of a small number of color-blended highlights.

4 Experimental Results

Experimental Conditions. We have conducted several experiments on real images. We used a SONY DXC-9000, a progressive 3 CCD digital camera, setting its gamma correction off. To ensure that the outputs of the camera would be linear to the flux of incident light, we used a spectrometer: Photo Research PR-650. We tested the algorithm by using three types of surfaces, i.e., uniform colored surfaces, multicolored surfaces, and highly textured surfaces. All target objects had a convex shape to avoid interreflection, and saturated pixels were excluded from the computation. For evaluation, we compared the results with the average values of image chromaticity of a white reference image (Photo Research Reflectance Standard model SRS-3), captured by the same camera. The standard deviations of these average

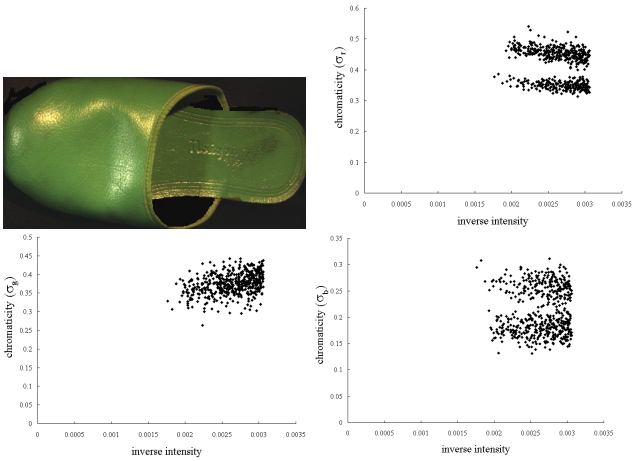

Figure 9: a. Real input image of a green sandal (uniformly colored surface). b. Result of projecting the specular pixels into inverse-intensity chromaticity space, with σ_c representing the red channel. c. Result of projecting the specular pixels, with σ_c representing the green channel. d. Result of projecting the specular pixels, with σ_c representing the blue channel.

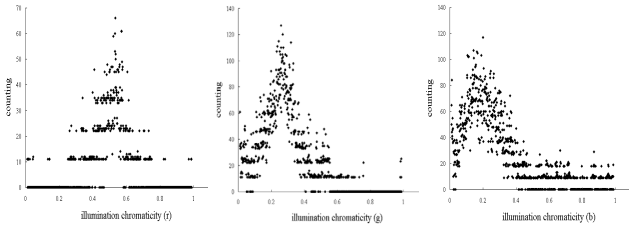

Figure 10: First iteration: a. intersection counting distribution for red channel of illumination chromaticity in Figure 9. b. Intersection counting distribution for green-channel c. Intersection counting distribution for blue channel.

values under various illuminant positions and colors were approximately $0.01 \sim 0.03$.

Result on a uniform colored surface. Figure 9.a shows a real image of a green sandal with uniformly colored surface. The sandal was lit by two illuminants: an incandescent lamp and a Solux halogen lamp. Under the illuminations, the image chromaticity of the white reference taken by our camera has chromaticity value: $\Gamma_r = 0.503, \Gamma_g = 0.298, \Gamma_b = 0.199$ for the incandescent light and $\Gamma_r = 0.371, \Gamma_g = 0.318, \Gamma_b = 0.310$ for the Solux halogen lamp.

Figure 9.b $\sim$ d show the first projection of highlight regions into inverse-intensity space. The intersection distribution in the Hough space is shown in Figure 10.a $\sim$ c. Having obtained the highest count in the red channel(the red channel of first illumination chromaticity), we detect the cluster lit by the illumination. The detection result is represented by brighter clusters in Figure 11.a $\sim$ c. By removing these clusters, we continue to the second iteration. The second illumination chromaticity can be found from the intersection counting distribution shown in Figure 12. The estimation results are: $\Gamma_r = 0.516, \Gamma_g = 0.279, \Gamma_b = 0.174$ for the incandescent light and $\Gamma_r = 0.400, \Gamma_g = 0.262, \Gamma_b = 0.324$ for the Solux halogen lamp.

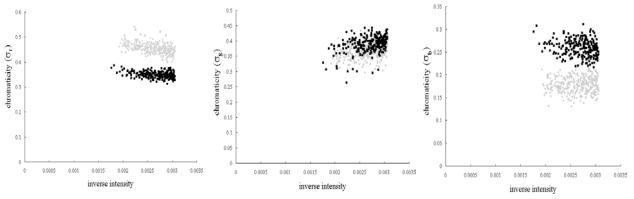

Figure 11: Second iteration: a. result of projecting the specular pixels into inverse-intensity chromaticity space, with σ_c representing the red channel. b. Result of projecting the specular pixels, with σ_c representing the green channel. c. Result of projecting the specular pixels, with σ_c representing the blue channel.

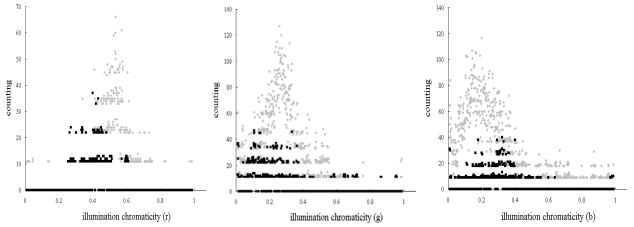

Figure 12: Second iteration: a. Intersection counting distribution for red channel of illumination chromaticity in Figure 11. b. Intersection counting distribution for green-channel c. Intersection counting distribution for blue channel.

Result on multicolored surface. Figure 13.a shows an image of a multicolored object. The object was illuminated by two illuminants: an incandescent lamp and a Solux halogen lamp. Under the illuminations, the image chromaticity of the white reference taken by our camera has chromaticity value: $\Gamma_r = 0.503, \Gamma_g = 0.298, \Gamma_b = 0.199$ for the incandescent light and $\Gamma_r = 0.371, \Gamma_g = 0.318, \Gamma_b = 0.310$ for the Solux halogen lamp.

Figure 13.b $\sim$ d show the first projection of highlight regions into inverse-intensity space. The intersection distribution in the Hough space is shown in Figure 14.a $\sim$ c. After obtaining the highest count in the red channel (the red channel of the first illumination chromaticity), we detected the cluster lit by the illumination. The detection result is represented by brighter clusters in Figure 15.a $\sim$ c. By removing these clusters, we continue to the second iteration. The second illumination chromaticity can be found from the intersection counting distribution shown in Figure 16. The estimation results are: $\Gamma_r = 0.513, \Gamma_g = 0.293, \Gamma_b = 0.157$ for the incandescent light and $\Gamma_r = 0.312, \Gamma_g = 0.454, \Gamma_b = 0.217$ for the Solux halogen lamp.

Result on highly textured surface. Figure 17.a shows an image of a highly textured surface. The object was illuminated by two illuminants: an incandescent lamp and a fluorescent lamp. Under the illuminations, the image chromaticity of the white reference taken by our camera has chromaticity value: $\Gamma_r = 0.4605, \Gamma_g = 0.362, \Gamma_b = 0.177$ for the incandescent light and $\Gamma_r = 0.340, \Gamma_g = 0.340, \Gamma_b = 0.319$ for the fluorescent lamp.

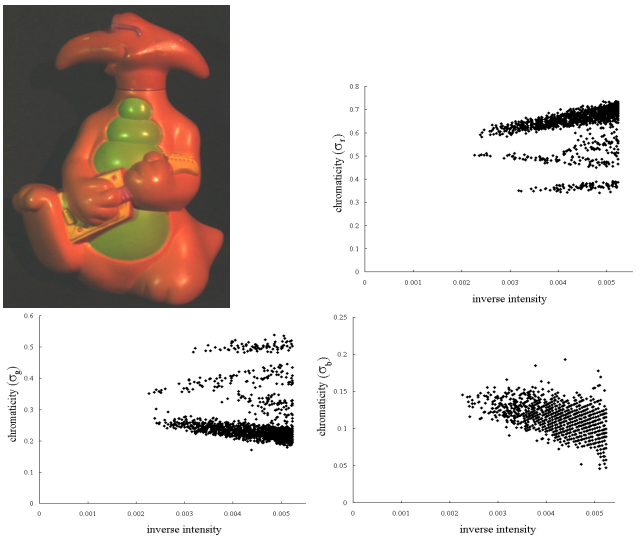

Figure 13: a. Real input image with multicolored surface. b. Result of projecting the specular pixels into inverse-intensity chromaticity space, with σ_c representing the red channel. c. Result of projecting the specular pixels, with σ_c representing the green channel. d. Result of projecting the specular pixels, with σ_c representing the blue channel.

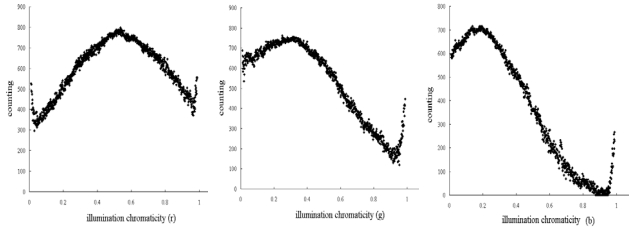

Figure 14: First iteration: a. Intersection counting distribution for the red channel of illumination chromaticity in Figure 13. b. Intersection counting distribution for the green-channel c. Intersection counting distribution for the blue channel.

Figure 17.b $\sim$ d show the first projection of highlighted regions into inverse-intensity space. The intersection distribution in the hough space is shown in Figure 18.a $\sim$ c. After obtaining the highest count in red channel (the red channel of the first illumination chromaticity), we detect the cluster lit by the illumination. The detection result is representing by brighter clusters in Figure 19.a $\sim$ c. By removing these clusters, we continue to the second iteration. The second illumination chromaticity can be found from the intersection counting distribution shown in Figure 20.The estimation results are: $\Gamma_r = 0.466, \Gamma_g = 0.3150, \Gamma_b = 0.209$ for the incandescent light and $\Gamma_r = 0.326, \Gamma_g = 0.305, \Gamma_b = 0.365$ for the fluorescence lamp.

5. Conclusion

We have introduced a method to estimate chromaticity of multicolored illuminations. Given rough highlight regions, the method does not require any further segmentation, and will work for all possible colors of illumination. The main idea of the method is the iterative algorithm in inverse-intensity space, Hough space, and histogram analysis. The experimental results have demonstrated that the method is effective even for highly textured surfaces.

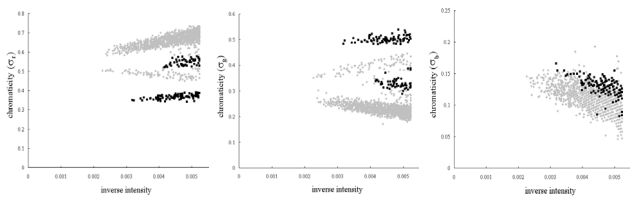

Figure 15: Second iteration: a. Result of projecting the specular pixels into inverse-intensity chromaticity space, with σ_c representing the red channel. b. Result of projecting the specular pixels, with σ_c representing the green channel. c. Result of projecting the specular pixels, with σ_c representing the blue channel.

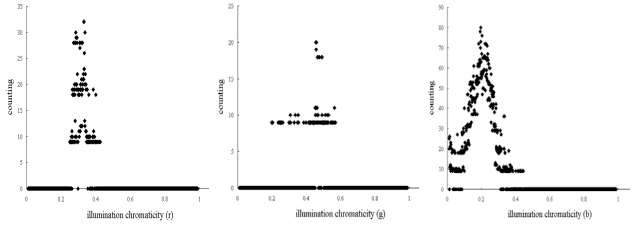

Figure 16: Second iteration: a. Intersection counting distribution for the red channel of illumination chromaticity in Figure 15. b. Intersection counting distribution for the green-channel c. Intersection counting distribution for the blue channel.

Acknowledgements

This research was, in part, supported by Japan Science and Technology (JST) under CREST Ikeuchi Project.

References

[1] H.J. Andersen and E. Granum. Classifying illumination conditions from two light sources by colour histogram assessment. *Journal of Optics Society of America A.*, 17(4):667–676, 2000.

[2] K. Barnard, G. Finlayson, and B. Funt. Color constancy for scenes with varying illumination. *Computer Vision and Image Understanding*, 65(2):311–321, 1997.

[3] D.H. Brainard and W.T. Freeman. Bayesian color constancy. *Journal of Optics Society of America A.*, 14(7):1393–1411, 1997.

[4] M. D'Zmura and P. Lennie. Mechanism of color constancy. *Journal of Optics Society of America A.*, 3(10):1162–1672, 1986.

[5] G.D. Finlayson. Color in perspective. *IEEE Trans. on Pattern Analysis and Machine Intelligence*, 18(10):1034–1038, 1996.

[6] G.D. Finlayson and B.V. Funt. Color constancy using shadows. *Perception*, 23:89–90, 1994.

[7] G.D. Finlayson, B.V. Funt, and K. Barnard. Color constancy under varying illumination. *International Conference on Computer Vision*, pages 720–725, 1995.

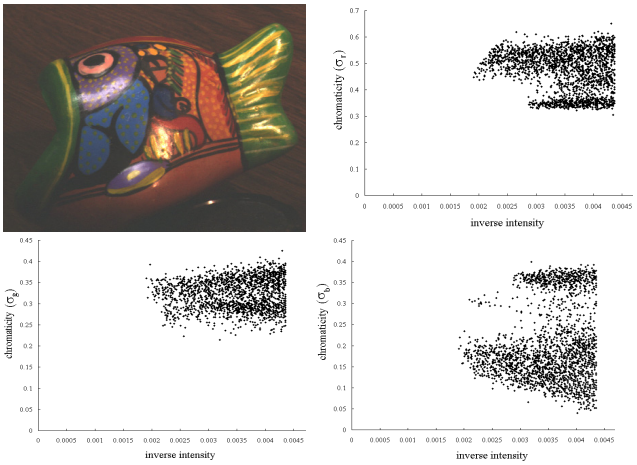

Figure 17: a. Real input image with highly textured surface. b. Result of projecting the specular pixels into inverse-intensity chromaticity space, with σ_c representing the red channel. c. Result of projecting the specular pixels, with σ_c representing the green channel. d. Result of projecting the specular pixels, with σ_c representing the blue channel.

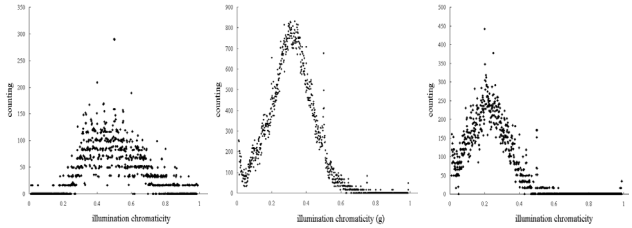

Figure 18: a. Intersection counting distribution for the red channel of illumination chromaticity in Figure 17. b. Intersection counting distribution for the green-channel c. Intersection counting distribution for the blue channel.

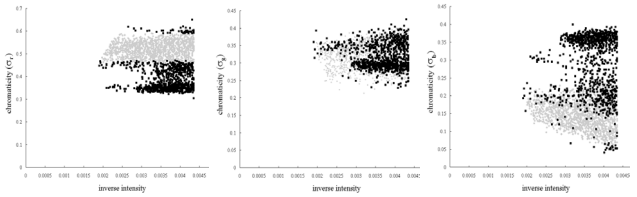

Figure 19: a. Result of projecting the specular pixels into inverse-intensity chromaticity space, with σ_c representing the red channel. b. Result of projecting the specular pixels, with σ_c representing the green channel. c. Result of projecting the specular pixels, with σ_c representing the blue channel.

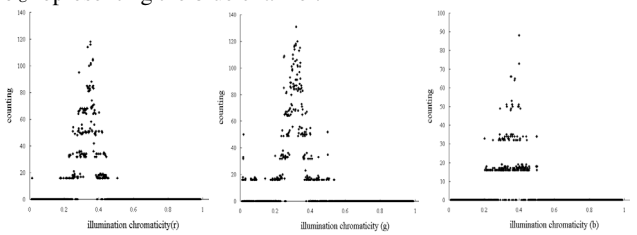

Figure 20: a. Intersection counting distribution for the red channel of illumination chromaticity in Figure 19. b. Intersection counting distribution for the green-channel c. Intersection counting distribution for the blue channel.

[8] G.D. Finlayson, S.D. Hordley, and P.M. Hubel. Color by correlation: a simple, unifying, framework for color constancy. *IEEE Trans. on Pattern Analysis and Machine Intelligence*, 23(11):1209–1221, 2001.

[9] G.D. Finlayson and G. Schaefer. Convex and non-convex illumination constraints for dichromatic color constancy. In *Conference on Computer Vision and Pattern Recognition*, volume I, page 598, 2001.

[10] G.D. Finlayson and G. Schaefer. Solving for color constancy using a constrained dichromatic reflection model. *International Journal of Computer Vision*, 42(3):127–144, 2001.

[11] J.M. Geusebroek, R. Boomgaard, S. Smeulders, and H. Geert. Color invariance. *IEEE Trans. on Pattern Analysis and Machine Intelligence*, 23(12):1338–1350, 2001.

[12] J.M. Geusebroek, R. Boomgaard, S. Smeulders, and T. Gevers. A physical basis for color constancy. In *The First European Conference on Colour in Graphics, Image and Vision*, pages 3–6, 2002.

[13] G.J. Klinker, S.A. Shafer, and T. Kanade. The measurement of highlights in color images. *International Journal of Computer Vision*, 2:7–32, 1990.

[14] E.H. Land and J.J. McCann. Lightness and retinex theory. *Journal of Optics Society of America*, 61(1):1–11, 1971.

[15] H.C. Lee. Method for computing the scene-illuminant from specular highlights. *Journal of Optics Society of America A.*, 3(10):1694–1699, 1986.

[16] H.C. Lee. Illuminant color from shading. In *Perceiving, Measuring and Using Color*, page 1250, 1990.

[17] T.M. Lehmann and C. Palm. Color line search for illuminant estimation in real-world scene. *Journal of Optics Society of America A.*, 18(11):2679–2691, 2001.

[18] C. Rosenberg, M. Hebert, and S. Thrun. Color constancy using kl-divergence. In *International Conference on Computer Vision*, volume I, page 239, 2001.

[19] S. Shafer. Using color to separate reflection components. *Color Research and Applications*, 10:210–218, 1985.

[20] R.T. Tan, K. Nishino, and K. Ikeuchi. Illumination chromaticity estimation using inverse-intensity chromaticity space. *in proceeding of IEEE Computer Society Conference on Computer Vision and Pattern Recognition (CVPR)*, pages 673–680, 2003.

[21] S. Tominaga. A multi-channel vision system for estimating surface and illumination functions. *Journal of Optics Society of America A.*, 13(11):2163–2173, 1996.

[22] S. Tominaga, S. Ebisui, and B.A. Wandell. Scene illuminant classification: brighter is better. *Journal of Optics Society of America A.*, 18(1):55–64, 2001.

[23] S. Tominaga and B.A. Wandell. Standard surface-reflectance model and illumination estimation. *Journal of Optics Society of America A.*, 6(4):576–584, 1989.

[24] K.E. Torrance and E.M. Sparrow. Theory for off-specular reflection from roughened surfaces. *Journal of Optics Society of America*, 57:1105–1114, 1966.